

Malignant hyperthermia susceptibility arising from altered resting coupling between the skeletal muscle L-type Ca²⁺ channel and the type 1 ryanodine receptor

Jose Miguel Eltit^{a,b,1}, Roger A. Bannister^{c,1}, Ong Moua^d, Francisco Altamirano^e, Philip M. Hopkins^f, Isaac N. Pessah^g, Tadeusz F. Molinski^h, Jose R. López^a, Kurt G. Beam^{d,2}, and Paul D. Allen^a

^aDepartment of Anesthesiology, Perioperative and Pain Medicine, Brigham and Women's Hospital, Harvard Medical School, Boston, MA 02115; ^bDepartment of Physiology and Biophysics, School of Medicine, Virginia Commonwealth University, Richmond, VA 23298; ^cCardiology Division, Department of Medicine, and ^dDepartment of Physiology and Biophysics, School of Medicine, University of Colorado Denver–Anschutz Medical Campus, Aurora, CO 80045; ^eCentro de Estudios Moleculares de la Célula, Instituto de Ciencias Biomédicas, Facultad de Medicina, Universidad de Chile, Santiago, Chile 8380453; ^fMalignant Hyperthermia Investigation Unit, Leeds Institute of Molecular Medicine, St. James's University Hospital, Leeds LS9 7TF, United Kingdom; ^gDepartment of Molecular Biosciences, Center for Children's Environmental Health and Disease Prevention, School of Veterinary Medicine, University of California, Davis, CA 95616; and ^hDepartment of Chemistry and Biochemistry and Skaggs School of Pharmacy and Pharmaceutical Sciences, University of California at San Diego, La Jolla, CA 92093

Edited by Clara Franzini-Armstrong, University of Pennsylvania Medical Center, Philadelphia, PA, and approved April 3, 2012 (received for review November 22, 2011)

Malignant hyperthermia (MH) susceptibility is a dominantly inherited disorder in which volatile anesthetics trigger aberrant Ca²⁺ release in skeletal muscle and a potentially fatal rise in perioperative body temperature. Mutations causing MH susceptibility have been identified in two proteins critical for excitation–contraction (EC) coupling, the type 1 ryanodine receptor (RyR1) and Ca_v1.1, the principal subunit of the L-type Ca²⁺ channel. All of the mutations that have been characterized previously augment EC coupling and/or increase the rate of L-type Ca²⁺ entry. The Ca_v1.1 mutation R174W associated with MH susceptibility occurs at the innermost basic residue of the IS4 voltage-sensing helix, a residue conserved among all Ca_v channels [Carpenter D, et al. (2009) *BMC Med Genet* 10:104–115]. To define the functional consequences of this mutation, we expressed it in *dysgenic* (Ca_v1.1 null) myotubes. Unlike previously described MH-linked mutations in Ca_v1.1, R174W ablated the L-type current and had no effect on EC coupling. Nonetheless, R174W increased sensitivity of Ca²⁺ release to caffeine (used for MH diagnostic in vitro testing) and to volatile anesthetics. Moreover, in Ca_v1.1 R174W-expressing myotubes, resting myoplasmic Ca²⁺ levels were elevated, and sarcoplasmic reticulum (SR) stores were partially depleted, compared with myotubes expressing wild-type Ca_v1.1. Our results indicate that Ca_v1.1 functions not only to activate RyR1 during EC coupling, but also to suppress resting RyR1-mediated Ca²⁺ leak from the SR, and that perturbation of Ca_v1.1 negative regulation of RyR1 leak identifies a unique mechanism that can sensitize muscle cells to MH triggers.

1,4-dihydropyridine receptor | α_{1S}

Malignant hyperthermia (MH) is a potentially fatal, pharmacogenetic disorder that can be triggered by depolarizing muscle relaxants or halogenated anesthetics (1). Following exposure to one of these triggers, MH-susceptible individuals enter a hypermetabolic crisis characterized by tachycardia, muscle rigidity, rhabdomyolysis, increased oxidative/nitrosative stress, mitochondrial damage, acidosis, hypercapnia, and renal failure leading ultimately to death. Currently, the only means to pharmacologically terminate an MH crisis is immediate administration of the hydantoin derivative dantrolene (2).

MH has long been linked to defective excitation–contraction (EC) coupling in skeletal muscle (3). Ordinarily, EC coupling in skeletal muscle occurs in response to depolarization of the plasma membrane, which causes conformational changes of L-type Ca²⁺ channels containing Ca_v1.1 as the principal subunit (4–6). These voltage-dependent conformational changes result in (i) activation of the L-type Ca²⁺ current and (ii) the activation of

Ca²⁺ release from the sarcoplasmic reticulum (SR) via type 1 ryanodine receptors (RyR1). Importantly, activation of RyR1 in skeletal muscle does not depend on the L-type Ca²⁺ current but, rather, is linked directly to the conformational changes of the L-type channels (“conformational coupling”) (4, 7, 8).

The vast majority of mutations (>180) associated with MH lie in the gene encoding RyR1 (9), but three individual mutations have been identified in the gene encoding Ca_v1.1 (10–13). Previously characterized mutations in either channel have been found to promote activation of RyR1 during EC coupling and/or to enhance Ca²⁺ entry via Ca_v1.1 (13–21). Thus, it has been proposed that augmented Ca²⁺ movements via the EC coupling pathway or via the L-type current underlie the fulminant response to MH triggers.

In this study, we describe the unexpected functional consequences of the recently identified R174W MH-causing mutation in Ca_v1.1 (10). In particular, we have found that the R174W mutation ablates activation of the L-type Ca²⁺ current but has surprisingly little effect on the Ca_v1.1-dependent activation of RyR1 Ca²⁺ release in response to depolarization. Strikingly, however, *dysgenic* (Ca_v1.1 null) myotubes expressing Ca_v1.1 R174W had elevated resting myoplasmic Ca²⁺ levels, depressed SR Ca²⁺ store content, and a greatly increased sensitivity to volatile anesthetics. Thus, it appears that the R174W mutation perturbs resting coupling between Ca_v1.1 and RyR1, promoting RyR1 leak (22), and that altered resting coupling represents a unique mechanism for the pathogenesis of MH.

Results

R174W Mutation in Ca_v1.1 Ablates L-Type Ca²⁺ Current. Because the R174W mutation occurs at a highly conserved position in a region of Ca_v1.1 (IS4) known to be important in sensing changes in membrane potential (23, 24), we first examined whether the R174W mutation affected the ability of Ca_v1.1 to function as an L-type Ca²⁺ channel. For this, we constructed a YFP-Ca_v1.1 R174W fusion construct and expressed the mutant channel in *dysgenic*

Author contributions: J.M.E., R.A.B., P.M.H., I.N.P., J.R.L., K.G.B., and P.D.A. designed research; J.M.E., R.A.B., O.M., F.A., and J.R.L. performed research; T.F.M. contributed new reagents/analytic tools; J.M.E., R.A.B., I.N.P., J.R.L., K.G.B., and P.D.A. analyzed data; and J.M.E., R.A.B., I.N.P., J.R.L., K.G.B., and P.D.A. wrote the paper.

The authors declare no conflict of interest.

This article is a PNAS Direct Submission.

¹J.M.E. and R.A.B. contributed equally to this work.

²To whom correspondence should be addressed. E-mail: kurt.beam@UCDenver.edu.

This article contains supporting information online at www.pnas.org/lookup/suppl/doi:10.1073/pnas.1119207109/-DCSupplemental.

(effectively $\text{Ca}_v1.1$ null) myotubes. Remarkably, YFP- $\text{Ca}_v1.1$ R174W yielded no inward Ca^{2+} current under our standard recording conditions ($n = 7$; Fig. 1A) even though the fluorescence arising from the YFP tag indicated normal expression and targeting of the mutant channel (Fig. S1). In contrast to YFP- $\text{Ca}_v1.1$, which predictably produced robust L-type current (-6.1 ± 0.7 pA/pF at +50 mV, $n = 32$; Fig. 1B), YFP- $\text{Ca}_v1.1$ R174W had an $I-V$ relationship that was nearly superimposable on that of naive *dysgenic* myotubes (Fig. 1C and Table S1). To determine whether the absence of L-type current in YFP- $\text{Ca}_v1.1$ R174W-expressing myotubes was a consequence of fewer channels present in the membrane, we recorded intramembrane charge movements. Myotubes expressing YFP- $\text{Ca}_v1.1$ R174W produced maximal charge movement (6.5 ± 0.7 nC/ μF , $n = 7$; Fig. 1D) that was similar to that of YFP- $\text{Ca}_v1.1$ -expressing myotubes (7.6 ± 0.9 nC/ μF , $n = 12$; $P > 0.05$, unpaired t test; Fig. 1E and Table S1) and was substantially larger than that of naive *dysgenic* myotubes (1.6 ± 0.2 nC/ μF , $n = 6$; $P < 0.001$, ANOVA; Fig. 1F and Table S1). Thus, the absence of L-type current in YFP- $\text{Ca}_v1.1$ R174W-expressing

myotubes was not a consequence of poor membrane expression of the mutant channel. We observed no clear difference in the voltage dependence of charge movement between YFP- $\text{Ca}_v1.1$ - and YFP- $\text{Ca}_v1.1$ R174W-expressing myotubes ($V_O = -7.4 \pm 2.0$ vs. -6.4 ± 2.4 mV, respectively; $P > 0.05$, unpaired t test; Fig. 1F and Table S1).

EC Coupling Is Little Affected by the $\text{Ca}_v1.1$ R174W Mutation. To determine whether the R174W mutation altered EC coupling, as has been demonstrated for other MH-causing mutations in either RyR1 (14–20, 25–27) or $\text{Ca}_v1.1$ (21), we measured myoplasmic Ca^{2+} transients in the whole-cell configuration. As shown in Fig. 2A, *dysgenic* myotubes expressing YFP- $\text{Ca}_v1.1$ produced robust Ca^{2+} transients with a mean $\Delta F/F_{\text{max}}$ of 1.82 ± 0.63 ($n = 11$) and an activation midpoint (V_F) of 14.0 ± 2.5 mV. *Dysgenic* myotubes expressing YFP- $\text{Ca}_v1.1$ R174W yielded Ca^{2+} transients that were similar both in magnitude ($\Delta F/F_{\text{max}} = 1.85 \pm 0.49$, $n = 6$; $P > 0.05$, unpaired t test; Fig. 2B and C and Table S2) and in voltage dependence ($V_F = 10.1 \pm 1.5$ mV; $P > 0.05$, unpaired t test; Table S2).

As an additional means to study possible alterations in the ability of $\text{Ca}_v1.1$ R174W to engage EC coupling, we created cell lines stably expressing either wild-type $\text{Ca}_v1.1$ or $\text{Ca}_v1.1$ R174W from *dysgenic* progenitor cells (Fig. S2). Myoplasmic Ca^{2+} transients in these cells were measured in response to depolarization

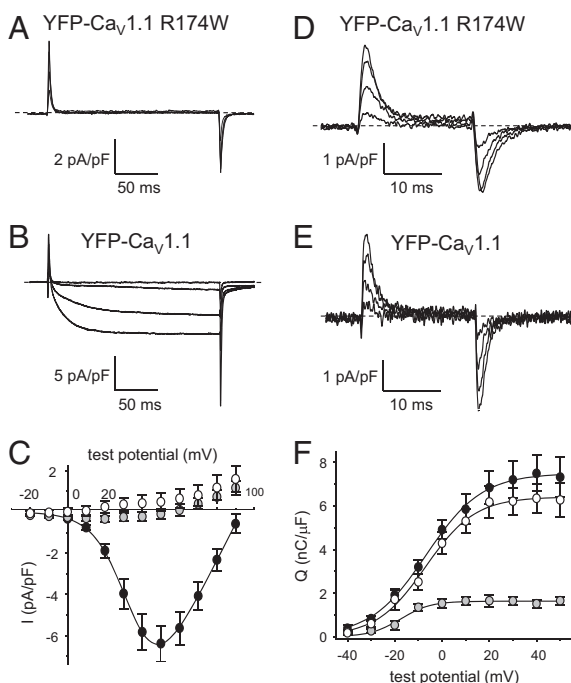


Fig. 1. Ca^{2+} currents and charge movements recorded from primary *dysgenic* myotubes expressing either YFP- $\text{Ca}_v1.1$ or YFP- $\text{Ca}_v1.1$ R174W. (A and B) Representative currents evoked from -50 mV to -10 , 10 , 30 , and 50 mV are shown for *dysgenic* myotubes expressing either YFP- $\text{Ca}_v1.1$ R174W (A) or YFP- $\text{Ca}_v1.1$ (B). (C) Peak $I-V$ relationships for naive *dysgenic* myotubes (\bullet ; $n = 8$) or *dysgenic* myotubes expressing either YFP- $\text{Ca}_v1.1$ (\bullet ; $n = 32$) or YFP- $\text{Ca}_v1.1$ R174W (\circ ; $n = 7$). In the case of YFP- $\text{Ca}_v1.1$ R174W, $I-V$ data were collected only from the 7 myotubes where channel expression was confirmed by charge movement; no inward current was observed in 10 additional *dysgenic* myotubes displaying yellow fluorescence. Currents were evoked at 0.1 Hz by test potentials ranging from -20 mV through $+90$ mV in 10 -mV increments, following a prepulse protocol (41). Current amplitudes were normalized by linear cell capacitance (pA/pF). The smooth curve for YFP- $\text{Ca}_v1.1$ is plotted according to Eq. 1, with best-fit parameters presented in Table S1. (D and E) Representative charge movements evoked from -50 mV to -30 , -10 , 10 , and 30 mV are shown for *dysgenic* myotubes expressing either YFP- $\text{Ca}_v1.1$ R174W (D) or YFP- $\text{Ca}_v1.1$ (E). Charge movements were evoked at 0.1 Hz by test potentials ranging from -40 mV through $+50$ mV in 10 -mV increments following a prepulse protocol. (F) $Q-V$ relationships for naive *dysgenic* myotubes ($n = 6$) or *dysgenic* myotubes expressing either YFP- $\text{Ca}_v1.1$ ($n = 12$) or YFP- $\text{Ca}_v1.1$ R174W ($n = 7$). The smooth curves are plotted according to Eq. 2, with respective best-fit parameters presented in Table S1.

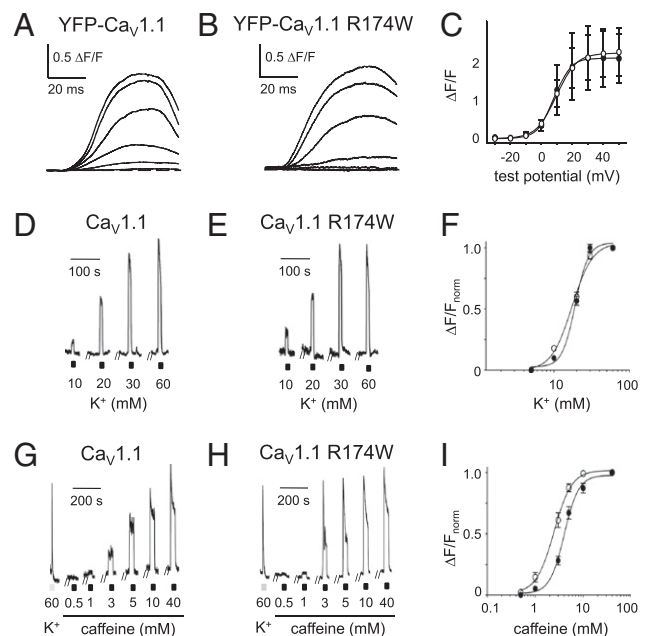


Fig. 2. The R174W mutation has little effect on the ability of $\text{Ca}_v1.1$ to function as the voltage sensor for EC coupling. (A and B) Recordings of myoplasmic Ca^{2+} transients elicited by 50 -ms depolarizations from -50 mV to -20 , -10 , 0 , 10 , 20 , and 30 mV are shown for *dysgenic* myotubes expressing either YFP- $\text{Ca}_v1.1$ (A) or YFP- $\text{Ca}_v1.1$ R174W (B). (C) Average $\Delta F/F_{\text{max}}$ relationships for *dysgenic* myotubes expressing either YFP- $\text{Ca}_v1.1$ (\bullet ; $n = 11$) or YFP- $\text{Ca}_v1.1$ R174W (\circ ; $n = 7$) fitted by Eq. 3 with the parameters presented in Table S1. (D and E) Representative elevated K^+ -induced Ca^{2+} transients in *dysgenic* myotubes stably expressing wild-type $\text{Ca}_v1.1$ (D) or $\text{Ca}_v1.1$ R174W (E). (F) K^+ dose-response relationships for *dysgenic* myotubes stably expressing either wild-type $\text{Ca}_v1.1$ ($n = 19$) or $\text{Ca}_v1.1$ R174W ($n = 32$) fitted by Eq. 4. (G and H) Representative caffeine-induced Ca^{2+} transients in *dysgenic* myotubes stably expressing $\text{Ca}_v1.1$ (G) or $\text{Ca}_v1.1$ R174W (H). At the beginning of each experiment, myotubes were exposed to K^+ (60 mM) for 10 s to confirm either wild-type or mutant $\text{Ca}_v1.1$ expression. (I) Caffeine dose-response relationships for *dysgenic* myotubes stably expressing either wild-type $\text{Ca}_v1.1$ ($n = 24$) or $\text{Ca}_v1.1$ R174W ($n = 28$) fitted by Eq. 4.

by elevated extracellular K^+ . In these experiments, myotubes expressing either $Ca_v1.1$ or $Ca_v1.1$ R174W displayed virtually identical responses to elevated K^+ ($EC_{50} = 18.9 \pm 0.6$ mM, $n = 19$, and 18.0 ± 0.9 mM, $n = 31$, respectively; $P > 0.05$, t test; Fig. 2 D–F). Thus, the R174W mutation ablates the ability of $Ca_v1.1$ to conduct L-type Ca^{2+} current but has little, if any, effect on its function to serve as the voltage sensor for EC coupling.

Hypersensitivity to the RyR1 agonist caffeine in the in vitro contracture test (IVCT) is a benchmark diagnostic assay for MH susceptibility (3, 28). For this reason, we assessed the caffeine sensitivities of wild-type $Ca_v1.1$ - and $Ca_v1.1$ R174W-expressing myotubes. At the beginning of each experiment, myotubes were first exposed to a 60-mM K^+ challenge to confirm channel expression. Then, myotubes were exposed to progressively higher concentrations of caffeine to elicit Ca^{2+} release from the SR (Fig. 2 G and H). As would be expected for MH-susceptible muscle (10, 29), $Ca_v1.1$ R174W-expressing myotubes were more sensitive to caffeine ($EC_{50} = 2.6 \pm 0.2$ mM, $n = 28$) than myotubes expressing $Ca_v1.1$ ($EC_{50} = 4.8 \pm 0.4$ mM, $n = 24$; $P < 0.001$, t test; Fig. 2I).

Dysgenic Myotubes Expressing $Ca_v1.1$ R174W Have Elevated Resting Ca^{2+} Levels and Are More Sensitive to MH Triggers. Despite ablating L-type Ca^{2+} current and having no discernible effect on EC coupling, the R174W mutation surprisingly resulted in an elevation of resting myoplasmic Ca^{2+} (Fig. 3). As measured with Ca^{2+} -selective microelectrodes, $Ca_v1.1$ R174W-expressing myotubes had an average resting Ca^{2+} concentration that was nearly twice that observed in myotubes expressing wild-type $Ca_v1.1$ (234 ± 4 nM, $n = 33$ vs. 120 ± 1 nM, $n = 18$, respectively; $P < 0.001$, unpaired t test) and similar to those previously reported for other MH susceptibility genotypes (30). The mutation also altered the effects of known MH triggers on Ca^{2+} levels. In wild-type $Ca_v1.1$ -expressing myotubes, neither isoflurane nor the more potent halothane (both 0.1% by volume) caused a change in myoplasmic Ca^{2+} (120 ± 1 nM, $n = 15$ and 121 ± 2 nM, $n = 12$, respectively; $P > 0.05$, ANOVA; Fig. 3). In stark contrast, these volatile anesthetics caused myoplasmic Ca^{2+} in $Ca_v1.1$ R174W-expressing myotubes to increase by nearly fivefold (863 ± 21 nM, $n = 8$ and $1,234 \pm 21$ nM, $n = 10$, respectively; $P < 0.001$, ANOVA; Fig. 3). We next investigated whether a partially depleted SR Ca^{2+} store was associated with the elevation in resting myoplasmic Ca^{2+} , by exposing myotubes to ionomycin ($5 \mu\text{M}$) in a nominally Ca^{2+} -free medium (22). As shown in Fig. 4, the content of the SR Ca^{2+} store was less in $Ca_v1.1$ R174W-expressing myotubes than in those expressing wild-type $Ca_v1.1$

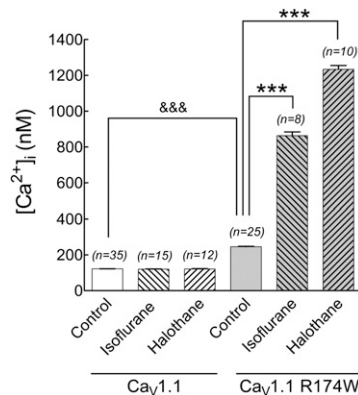


Fig. 3. Dysgenic myotubes expressing $Ca_v1.1$ R174W (Right) display elevated resting myoplasmic Ca^{2+} and hypersensitivity to MH triggers compared with dysgenic myotubes expressing wild-type $Ca_v1.1$ (Left). Myoplasmic Ca^{2+} levels measured with Ca^{2+} -sensitive microelectrodes are shown before (control) and after exposure to either isoflurane (0.1% vol/vol; Right, hatched bar) or halothane (0.1% vol/vol; Left, hatched bar). &&&, significant difference ($P < 0.001$, ANOVA) in resting Ca^{2+} between wild-type $Ca_v1.1$ and $Ca_v1.1$ R174W control groups. ***, significant ($P < 0.001$, ANOVA) difference between control and anesthetic-treated $Ca_v1.1$ R174W-expressing myotubes. In dysgenic myotubes expressing wild-type $Ca_v1.1$, no significant changes in myoplasmic Ca^{2+} were observed following exposure to the volatile anesthetics relative to control.

(integrated area under transient = 16.21 ± 3.05 arbitrary fluorescence units (afu)-s, $n = 39$ and 31.94 ± 3.57 afu-s, $n = 33$, respectively; $P < 0.01$, t test), consistent with the idea that resting SR Ca^{2+} leak is increased by $Ca_v1.1$ R174W.

Application of the L-type channel antagonist nifedipine had little effect on resting Ca^{2+} in either wild-type $Ca_v1.1$ -expressing or $Ca_v1.1$ R174W-expressing myotubes (118 ± 3 nM, $n = 6$ and 238 ± 3 nM, $n = 6$, respectively; $P > 0.05$, ANOVA, in both cases; Table 1), suggesting that the elevated resting Ca^{2+} levels were not a consequence of depolarization-dependent $Ca_v1.1$ activity. On the other hand, exposure to dantrolene decreased resting Ca^{2+} in $Ca_v1.1$ R174W myotubes (94 ± 2 , $n = 10$; $P < 0.05$, ANOVA; Table 1) but produced little effect on resting Ca^{2+} in wild-type $Ca_v1.1$ -expressing myotubes (89 ± 1 , $n = 10$; $P > 0.05$, ANOVA; Table 1). Additionally, the elevation in resting Ca^{2+} was partially blocked by bastadin 5, obtained from the marine sponge *Ianthella basta* (Table 1) (31).

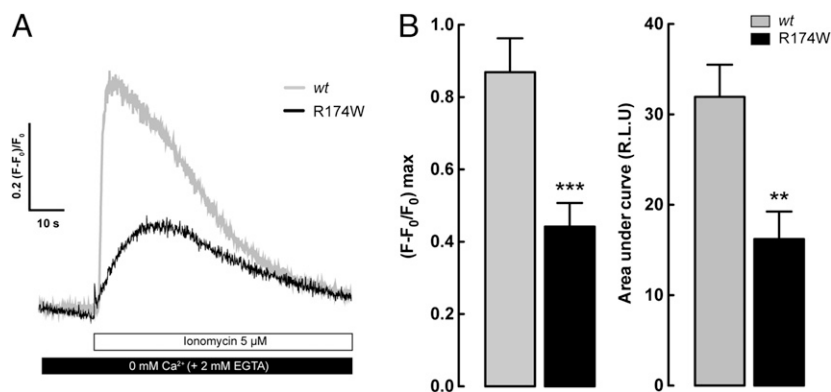


Fig. 4. SR Ca^{2+} store is partially depleted in $Ca_v1.1$ R174W-expressing dysgenic myotubes. (A) Representative ionomycin ($5 \mu\text{M}$)-induced Ca^{2+} transients in dysgenic myotubes stably expressing either wild-type $Ca_v1.1$ (shaded trace) or $Ca_v1.1$ R174W (solid trace). (B) Quantification of peak transient amplitude (Left) and integrated transient area (Right) for ionomycin-induced Ca^{2+} transients in dysgenic myotubes expressing $Ca_v1.1$ ($n = 33$) and $Ca_v1.1$ R174W ($n = 39$). Asterisks indicate significant differences (** $P < 0.01$; *** $P < 0.001$; unpaired t test).

Table 1. Myoplasmic Ca²⁺ measurements

	[Ca ²⁺] _{rest} nM	
	Ca _v 1.1	Ca _v 1.1 R174W
Control	120 ± 1 (18)	234 ± 4 (33)***
Nifedipine, 25 μM	118 ± 3 (6)	238 ± 3 (6)***
Dantrolene, 50 μM	89 ± 1 (10)&&&	94 ± 2 (10)&&&,NS
Bastadin 5, 10 μM	98 ± 2 (8)***&&&	171 ± 9 (8)***&&&

Data are given as mean ± SEM, with the numbers in parentheses indicating the number of myotubes tested. Control cells were exposed only to Imaging Solution (IS). Statistical differences: *** $P < 0.001$ vs. Ca_v1.1 (one-way ANOVA); &&& $P < 0.001$ vs. Ca_v1.1 R174W control. NS, no significant difference vs. Ca_v1.1 ($P > 0.05$, one-way ANOVA).

Discussion

The results reported here identify a mechanism for MH susceptibility fundamentally different from those ascribed to other MH-causing mutations, which either enhance entry of Ca²⁺ via the L-type channel or shift the equilibrium of RyR1 toward the activated (open) state. Importantly, we find that the R174W mutation does not alter the voltage dependence of EC coupling (Fig. 2), which indicates that this mutation does not shift the equilibrium of RyR1 toward the activated state. Furthermore, the mutation obviously does not promote L-type Ca²⁺ entry (Fig. 1). However, our results are consistent with the idea that the R174W mutation in Ca_v1.1 derepresses Ca²⁺ efflux from the SR in resting muscle cells. Thus, the Ca_v1.1–RyR1 interaction appears to have three manifestations: (i) Ca_v1.1-mediated engagement of EC coupling via RyR1, (ii) RyR1-dependent retrograde enhancement of L-type current via Ca_v1.1, and (iii) Ca_v1.1-mediated suppression of a resting SR Ca²⁺ leak via RyR1. Evidence for the last of these is provided by our previous work, which showed that resting SR Ca²⁺ stores are reduced, and myoplasmic Ca²⁺ levels are higher, in naive *dysgenic* (i.e., Ca_v1.1-lacking) myotubes compared with wild-type myotubes (22), suggesting that Ca_v1.1 represses a resting Ca²⁺ leak from the SR via RyR1 (Fig. 5A). The increase in resting myoplasmic Ca²⁺ in Ca_v1.1 R174W-expressing myotubes is also accompanied by a reduction in the resting SR Ca²⁺ store (Fig. 4). This leak pathway in *dysgenic* myotubes appears to be distinct from the conventional activated state of RyR1 because it is blocked by bastadin 5 (or bastadin 5 in the presence of ryanodine) but not by ryanodine alone (32, 33); bastadin 5 (B5) application also causes a partial reduction in resting myoplasmic Ca²⁺ in *dysgenic* myotubes expressing Ca_v1.1 R174W (Table 1). As shown in Fig. 5B, expression of wild-type Ca_v1.1 in *dysgenic* myotubes represses the resting Ca²⁺ leak (22) and restores both EC coupling and L-type current (6). The R174W mutation alters the resting conformation of Ca_v1.1 such that it no longer suppresses resting Ca²⁺ leak via RyR1 but does not noticeably alter its function as the voltage sensor for EC coupling (Fig. 5C). It should be pointed out that the level of resting Ca²⁺ in Ca_v1.1 R174W-expressing *dysgenic* myotubes (234 ± 4 nM; Table 1) is higher than that in naive *dysgenic* myotubes (163 ± 2.5 nM) (22), which suggests that in addition to removing block of the resting RyR1 leak, the R174W mutation also serves to amplify this resting leak.

Additional evidence supporting a causative role of resting leak in MH pathogenesis is that dantrolene, the clinical “antidote” for MH crises, restores resting Ca²⁺ to normal levels in *dysgenic* myotubes expressing Ca_v1.1 R174W (Table 1). Thus, our findings identify a unique mechanism underlying a potentially fatal human disorder. In particular, the R174W mutation disrupts the ability of Ca_v1.1 to repress resting Ca²⁺ leak from the SR via RyR1, leading to elevated resting myoplasmic Ca²⁺ and increased sensitivity to MH triggers. Significantly, elevations in resting myoplasmic Ca²⁺ that are not blocked by ryanodine have also been observed in *dyspedic* myotubes expressing eight distinct

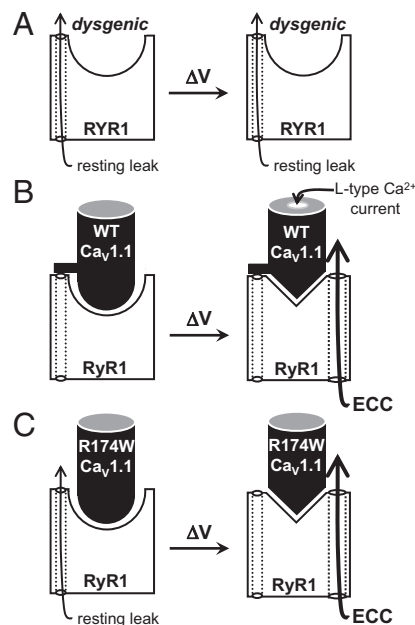


Fig. 5. The R174W mutation in Ca_v1.1 disrupts the resting interaction between Ca_v1.1 and RyR1 that suppresses Ca²⁺ leak from the SR. (A) Our previous work in *dysgenic* myotubes has demonstrated that the absence of Ca_v1.1 reveals a leak state of RyR1 (Left) that increases resting Ca²⁺ (22). Additionally, the absence of the Ca_v1.1 voltage sensor renders *dysgenic* myotubes incapable of EC coupling or generating L-type Ca²⁺ current during plasma membrane depolarization (Right) (42). (B) When present, Ca_v1.1 inhibits Ca²⁺ leak from the SR via RyR1 at rest (Left) and responds to depolarization by engaging EC coupling in Ca²⁺ release and producing L-type current (Right) (6). (C) The R174W mutation alters the conformation of Ca_v1.1 such that it does not suppress resting SR Ca²⁺ leak, leading to an increase in resting Ca²⁺ and enhanced sensitivity to MH triggers (Left; Fig. 3); the R174W mutation also ablates the ability of Ca_v1.1 to produce L-type current but has little, if any, effect on the ability of Ca_v1.1 to engage EC coupling (Right).

RyR1 MH-linked mutations (30). Thus, other mutations in either Ca_v1.1 or RyR1 may potentially lead to increased resting Ca²⁺ leak. Although increased SR Ca²⁺ leak may represent a sensitizing mechanism, it is almost certain that multiple mechanisms are at work in MH susceptibility. In this regard, any mechanism that causes sustained, partial SR Ca²⁺ store depletion would presumably result in a sustained increase in store-operated Ca²⁺ entry (34, 35) and thus increased resting myoplasmic Ca²⁺. Simply raising myoplasmic Ca²⁺ would be expected to increase the efficacy of other activators (e.g., caffeine and volatile anesthetics). Moreover, chronically elevated myoplasmic Ca²⁺ levels could have downstream sequelae as a result of altered mitochondrial metabolism (17, 36).

In conclusion, we have described a unique mechanism whereby a mutation of Ca_v1.1 promotes MH susceptibility by causing an increase in resting SR Ca²⁺ leak. It will be important to determine the extent to which an enhanced resting leak contributes to MH susceptibility for other Ca_v1.1 and RyR1 mutations.

Materials and Methods

Molecular Biology. YFP-Ca_v1.1 R174W was derived from the plasmid YFP-Ca_v1.1 (37), using the QuikChange II XL site-directed mutagenesis kit (Agilent Technologies).

Primary Culture and cDNA Expression. All procedures involving mice were approved by the Institutional Animal Care and Use Committees of University of Colorado Denver and Harvard Medical School. Primary cultures of *dysgenic* myotubes were prepared as described previously (38). Single nuclei of

differentiated myotubes were microinjected with 200 ng/ μ L plasmid cDNA encoding either YFP-Ca_v1.1 or YFP-Ca_v1.1 R174W.

Generation of Myoblasts Stably Expressing Wild-Type Ca_v1.1 or Ca_v1.1-R174W. cDNAs encoding either wild-type Ca_v1.1 (22) or Ca_v1.1 R174W were subcloned between the LTRs of a lentiviral vector driven by an EF1 α human promoter (22, 39). The lentiviral particles were packaged by transfection of HEK 293T cells as described previously (40). *Dysgenic* myoblasts were transduced with lentiviral particles and were replated with one cell per well in 96-well culture plates 24 h later. After 2–3 wk, myoblasts from 20–30 clones were plated in 96-well plates and differentiated into myotubes. To screen for expression of either Ca_v1.1 or Ca_v1.1 R174W, myotubes were loaded with Fluo-4 AM and challenged by K⁺ depolarization (see below); positive myotubes were identified by the ability to support Ca²⁺ transients in response to depolarization.

Electrophysiology. Electrophysiological experiments were performed with *dysgenic* myotubes expressing either YFP-Ca_v1.1 or YFP-Ca_v1.1 R174W 2 d postmicroinjection. Pipettes were fabricated from borosilicate glass and had resistances of ~2.0 M Ω when filled with internal solution, which consisted of 140 mM Cs-aspartate, 10 mM Cs₂-EGTA, 5 mM MgCl₂, and 10 mM Hepes, pH 7.4, with CsOH. The external solution contained 145 mM tetraethylammonium (TEA)-Cl, 10 mM CaCl₂, 0.002 mM tetrodotoxin, and 10 mM Hepes, pH 7.4, with TEA-OH. For measurement of charge movements, 0.5 mM CdCl₂ and 0.1 mM LaCl₃ were added to the external solution. Filtering was at 2 kHz (eight-pole Bessel filter; Frequency Devices) and digitization was either at 10 kHz (L currents) or 20 kHz (charge movements). Current–voltage (*I*–*V*) curves were fitted according to

$$I = G_{\max} * (V - V_{\text{rev}}) / \{1 + \exp[-(V - V_{1/2})/k_G]\}, \quad [1]$$

where *I* is the current for the test potential *V*, *V*_{rev} is the reversal potential, *G*_{max} is the maximum Ca²⁺ channel conductance, *V*_{1/2} is the half-maximal activation potential, and *k*_G is the slope factor. Plots of the integral of *Q*_{on} as a function of test potential (*V*) were fitted according to

$$Q_{\text{on}} = Q_{\max} / \{1 + \exp[(V_Q - V)/k_Q]\}, \quad [2]$$

where *Q*_{max} is the maximal *Q*_{on}, *V*_Q is the potential causing movement of half the maximal charge, and *k*_Q is a slope parameter.

Whole-Cell Measurement of Ca²⁺ Transients. Changes in intracellular Ca²⁺ were recorded with Fluo-3 (F-3715; Invitrogen). The dye was added to the internal solution for a final concentration of 200 μ M. After entry into the whole-cell configuration, a period of >5 min was used to allow the dye to diffuse into the cell interior. The peak fluorescence change ($\Delta F/F$) for each test potential (*V*) was fitted according to

$$\Delta F/F = [\Delta F/F]_{\max} / [1 + \exp\{-(V - V_F)/k_F\}], \quad [3]$$

where ($\Delta F/F$)_{max} is the maximal fluorescence change, *V*_F is the potential causing half the maximal change in fluorescence, and *k*_F is a slope parameter.

Intact Myotube Ca²⁺ Imaging. Differentiated *dysgenic* myotubes stably expressing wild-type Ca_v1.1 or Ca_v1.1 R174W were loaded with 5 μ M Fluo-4 AM (Invitrogen) for 15 min at 37 °C and washed with Imaging Solution (140 mM NaCl, 5 mM KCl, 1 mM MgCl₂, 1 mM CaCl₂, 5.5 mM glucose, 10 mM Hepes, pH 7.4, with NaOH). The Ca²⁺ signal was monitored using 480/30-nm excitation and 535/40-nm emission wavelengths. The peak response to a given K⁺ or caffeine concentration [$(\Delta F/F)_{\text{norm}}$] was quantified as the integrated area under the curve normalized by the maximal response to either agent (60 or 40 mM, respectively). Dose–response relationships were fit by the equation

$$(\Delta F/F)_{\text{norm}} = 1 / [1 + 10 \exp\{\log EC_{50} - \log X\} * k], \quad [4]$$

where EC₅₀ is the concentration that produces the half-maximal response, *X* is the concentration of K⁺ or caffeine applied, and *k* is a slope parameter.

Resting Myoplasmic Ca²⁺ Measurements. Resting myoplasmic Ca²⁺ levels in intact myotubes were assessed with double-barreled Ca²⁺-selective microelectrodes as described previously in ref. 22.

Assessment of SR Ca²⁺ Stores. *Dysgenic* myotubes stably expressing either wild-type Ca_v1.1 or Ca_v1.1 R174W were loaded with Fluo-4 AM (5 μ M) for 30 min at 37 °C and then incubated with nominally 0 mM Ca²⁺ Krebs Ringer solution supplemented with 2 mM EGTA. Ca²⁺ release from the SR was induced by the application of Krebs Ringer containing ionomycin (5 μ M) and quantified by the integrated area under the resultant Ca²⁺ transient. The Ca²⁺ signal was monitored using 480/30-nm excitation and 535/40-nm emission wavelengths; the emission signal was acquired at 30 frames per second.

Statistical Analysis. Figures were made using SigmaPlot 11.0 (SSPS). All data are presented as mean \pm SEM. Comparisons were made by unpaired, two-tailed *t* test or one-way ANOVA coupled with Tukey's *t* test (as appropriate), with *P* < 0.05 considered significant. A more complete description of experimental methods is included in *SI Materials and Methods*.

ACKNOWLEDGMENTS. This work was supported by National Institutes of Health Grants AR055104 (to K.G.B.), AR052534 (to P.D.A. and I.N.P.), and AG038778 (to R.A.B.) and Muscular Dystrophy Association Grant MDA176448 (to K.G.B.).

- Zhou J, Allen PD, Pessah IN, Naguib M (2009) Anesthesia, ed Miller RD (Churchill Livingstone, Philadelphia), pp 1033–1052.
- Krause T, Gerbershagen MU, Fiege M, Weisshorn R, Wappler F (2004) Dantrolene—a review of its pharmacology, therapeutic use and new developments. *Anaesthesia* 59:364–373.
- Avila G (2005) Intracellular Ca²⁺ dynamics in malignant hyperthermia and central core disease: Established concepts, new cellular mechanisms involved. *Cell Calcium* 37:121–127.
- Schneider MF, Chandler WK (1973) Voltage dependent charge movement of skeletal muscle: A possible step in excitation-contraction coupling. *Nature* 242:244–246.
- Rios E, Brum G (1987) Involvement of dihydropyridine receptors in excitation-contraction coupling in skeletal muscle. *Nature* 325:717–720.
- Tanabe T, Beam KG, Powell JA, Numa S (1988) Restoration of excitation-contraction coupling and slow calcium current in dysgenic muscle by dihydropyridine receptor complementary DNA. *Nature* 336:134–139.
- Armstrong CM, Bezanilla FM, Horowitz P (1972) Twitches in the presence of ethylene glycol bis(-aminoethyl ether)-N,N'-tetracetic acid. *Biochim Biophys Acta* 267:605–608.
- Dirksen RT, Beam KG (1999) Role of calcium permeation in dihydropyridine receptor function. Insights into channel gating and excitation-contraction coupling. *J Gen Physiol* 114:393–403.
- Robinson R, Carpenter D, Shaw M-A, Halsall J, Hopkins P (2006) Mutations in RYR1 in malignant hyperthermia and central core disease. *Hum Mutat* 27:977–989.
- Carpenter D, et al. (2009) The role of CACNA1S in predisposition to malignant hyperthermia. *BMC Med Genet* 10:104–115.
- Monnier N, Procaccio V, Stieglitz P, Lunardi J (1997) Malignant-hyperthermia susceptibility is associated with a mutation of the alpha 1-subunit of the human dihydropyridine-sensitive L-type voltage-dependent calcium-channel receptor in skeletal muscle. *Am J Hum Genet* 60:1316–1325.
- Toppin PJ, et al. (2010) A report of fulminant malignant hyperthermia in a patient with a novel mutation of the CACNA1S gene. *Can J Anaesth* 57:689–693.
- Pirone A, et al. (2010) Identification and functional characterization of malignant hyperthermia mutation T1354S in the outer pore of the Ca_v1.1 subunit. *Am J Physiol* 299:C1345–C1354.
- Dietze B, Henke J, Eichinger HM, Lehmann-Horn F, Melzer W (2000) Malignant hyperthermia mutation Arg615Cys in the porcine ryanodine receptor alters voltage dependence of Ca²⁺ release. *J Physiol* 526:507–514.
- Chelu MG, et al. (2006) Heat- and anesthesia-induced malignant hyperthermia in an RyR1 knock-in mouse. *FASEB J* 20:329–330.
- Cherednichenko G, et al. (2008) Enhanced excitation-coupled calcium entry in myotubes expressing malignant hyperthermia mutation R163C is attenuated by dantrolene. *Mol Pharmacol* 73:1203–1212.
- Durham WJ, et al. (2008) RyR1 S-nitrosylation underlies environmental heat stroke and sudden death in Y522S RyR1 knockin mice. *Cell* 133:53–65.
- Andronache Z, Hamilton SL, Dirksen RT, Melzer W (2009) A retrograde signal from RyR1 alters DHP receptor inactivation and limits window Ca²⁺ release in muscle fibers of Y522S RyR1 knock-in mice. *Proc Natl Acad Sci USA* 106:4531–4536.
- Bannister RA, et al. (2010) A malignant hyperthermia-inducing mutation in RYR1 (R163C): Consequent alterations in the functional properties of DHPR channels. *J Gen Physiol* 135:629–640.
- Estève E, et al. (2010) A malignant hyperthermia-inducing mutation in RYR1 (R163C): Alterations in Ca²⁺ entry, release, and retrograde signaling to the DHPR. *J Gen Physiol* 135:619–628.
- Weiss RG, et al. (2004) Functional analysis of the R1086H malignant hyperthermia mutation in the DHPR reveals an unexpected influence of the III-IV loop on skeletal muscle EC coupling. *Am J Physiol Cell Physiol* 287:C1094–C1102.
- Eltit JM, et al. (2011) Orthograde dihydropyridine receptor signal regulates ryanodine receptor passive leak. *Proc Natl Acad Sci USA* 108:7046–7051.
- Tanabe T, et al. (1987) Primary structure of the receptor for calcium channel blockers from skeletal muscle. *Nature* 328:313–318.

